

See discussions, stats, and author profiles for this publication at: <https://www.researchgate.net/publication/11243006>

High-Resolution Colocalization of Single Dye Molecules by Fluorescence Lifetime Imaging Microscopy

ARTICLE *in* ANALYTICAL CHEMISTRY · AUGUST 2002

Impact Factor: 5.64 · DOI: 10.1021/ac025576g · Source: PubMed

CITATIONS

81

READS

35

9 AUTHORS, INCLUDING:



Rainer Heintzmann

Leibniz Institute of Photonic Technology

102 PUBLICATIONS 4,056 CITATIONS

SEE PROFILE



Christoph Cremer

Universität Heidelberg

319 PUBLICATIONS 10,566 CITATIONS

SEE PROFILE

High-Resolution Colocalization of Single Dye Molecules by Fluorescence Lifetime Imaging Microscopy

Mike Heilemann,[†] Dirk P. Herten,[‡] Rainer Heintzmann,[§] Christoph Cremer,^{||} Christian Müller,[†] Philip Tinnefeld,[†] Kenneth D. Weston,[†] Jürgen Wolfrum,[†] and Markus Sauer^{*,†}

Physikalisch-Chemisches Institut, Universität Heidelberg, Im Neuenheimer Feld 253, 69120 Heidelberg, Germany, ATTO-TEC GmbH, Schanzenweg 50, 57076 Siegen, Germany, Max Planck Institute for Biophysical Chemistry, Am Fassberg 11, 37077 Göttingen, and Kirchhoff-Institut für Physik, Universität Heidelberg, Albert-Ueberle-Strasse 3–5, 69120 Heidelberg, Germany

Conventional fluorescence microscopy can be used to determine the positions of objects in space when those objects are separated by distances greater than several hundred nanometers, as restricted by the diffraction limit of light. Fluorescence microscopy/spectroscopy based on fluorescence resonance energy-transfer techniques can be used to measure separation distances below ~10 nm. To fill the gap between these fundamental limits, we have developed an alternative technique for high-resolution colocalization of fluorescent dyes. The technique is based on fluorescence lifetime imaging. Under favorable conditions, the method can be used to distinguish, and to measure the distance between, two dye molecules that are less than 30 nm apart. To demonstrate the method, lifetime images of a mixture of Cy5 and JF9 (rhodamine derivative) molecules statistically adsorbed on a glass surface were acquired and analyzed. Since these two molecular species differ in fluorescence lifetime (for Cy5, $\tau_f = 2.0$ ns, and for JF9, $\tau_f = 4.0$ ns), it is possible to assign the contribution of fluorescence of the two dye types to each image pixel using a pattern recognition technique. Since both dye types can be excited using the same laser wavelength, the measurement is free of chromatic aberrations. The results presented demonstrate the first high-precision distance measurements between single conventional fluorescent dyes based solely on fluorescence lifetime.

In modern chemical analysis, the isolation, identification, and characterization of a vast array of biologically relevant molecules have become routine. What is still challenging scientists the world over is discovering how these molecules are assembled within cells and their nuclei to form the fundamental molecular machines supporting living organisms.^{1,2} An important example is the

replication foci formed during the S phase of the cell cycle where DNA synthesis occurs.^{3,4} Another is the transcription factories where DNA is transcribed into RNA.^{5,6} The architecture of these assemblies is based on numerous nucleic acids and protein components,^{7–9} each of which has been identified and well characterized. Despite this detailed knowledge, much less is known, beyond speculation, about how the components are arranged in the assemblies and how the components move during their functioning. This underscores the need for novel optical methods that can determine the spatial relationships and dynamic interplay of the interacting biomolecules that are part of such molecular machines. Since the size of the functional units is typically in the range of several tens of nanometers,⁶ the methods we will describe are very relevant. They are also advantageous due to the extreme sensitivity, down to the level of single molecules, and the possibility to expand the analysis to three dimensions.¹⁰

To observe and study the organization of molecular machines in the cell, a tool is needed that can provide dynamic, in vivo, three-dimensional (3D) microscopic pictures of individual molecules with nanometer resolution. While single fluorescent molecules can be detected in solution,^{11–13} on surfaces or in gels,^{14,15} and in membranes of living cells^{16,17} with good signal-to-noise ratio (S/N) using confocal microscopy, the spatial resolution

(2) Lamond, A. I.; Earnshaw, W. C. *Science* **1998**, *280*, 547–553.

(3) Cook, P. R. *Science* **1999**, *284*, 1790–1795.

(4) Leonhardt, H.; Rahn, H. P.; Cardoso, M. C. *J. Cell. Biochem. Suppl.* **1998**, *30/31*, 243–249.

(5) Wansink, D. G.; Sibon, O. C.; Cremers, F. F.; van Driel, R.; de Long, L. J. *Cell Biochem.* **1996**, *62*, 10–18.

(6) Pombo, A.; Jackson, D. A.; Hollinshead, M.; Wang, Z.; Roeder, R. G.; Cook, P. R. *EMBO J.* **1999**, *18*, 2241–2253.

(7) Cardoso, M. C.; Leonhardt, H. *J. Cell. Biochem.* **1998**, *70*, 222–230.

(8) Cardoso, M. C.; Leonhardt, H.; Nadal-Ginard, B. *Cell* **1993**, *74*, 979–992.

(9) Jackson, D. A.; Iborra, F. J.; Manders, E. M. M.; Cook, P. R. *Mol. Biol. Cell* **1998**, *9*, 1523–1536.

(10) Pawley, J. B. *Handbook of Biological Confocal Microscopy*, 2nd ed; Plenum Press: New York, 1995.

(11) Mets, Ü.; Rigler, R. *J. Fluoresc.* **1994**, *4*, 259–264.

(12) Nie, S.; Chiu, N. T.; Zare, R. N. *Science* **1994**, *266*, 1018–1021.

(13) Ambrose, W. P.; Goodwin, P. M.; Jett, J. H.; van Orden, A.; Werner, H. J.; Keller, R. A. *Chem. Rev.* **1999**, *99*, 2929–2956.

(14) Weston, K. D.; Carson, P. J.; Metiu, H.; Buratto, S. K. *J. Chem. Phys.* **1998**, *109*, 7474–7484.

(15) Veerman, J. A.; Garcia-Parajo, M. F.; Kuipers, L.; van Hulst, N. F. *Phys. Rev. Lett.* **1999**, *83*, 2155–2157.

* Corresponding author: (e-mail) sauer@urz.uni-heidelberg.de; (phone) +49-6221-548460; (fax) +49-6221-544255.

[†] Physikalisch-Chemisches Institut, Universität Heidelberg.

[‡] ATTO-TEC GmbH.

[§] Max Planck Institute for Biophysical Chemistry.

^{||} Kirchhoff-Institut für Physik, Universität Heidelberg.

(1) Spector, D. L. *Annu. Rev. Cell Biol.* **1993**, *9*, 265–315.

is generally insufficient. In the past decade, significant advances have been made in improving the spatial resolution of optical microscopy beyond the classical diffraction limit of light. New methods include (i) 4Pi microscopy,¹⁸ (ii) near-field scanning optical microscopy (NSOM),¹⁹ and (iii) point-spread-function (PSF) engineering by stimulated emission depletion (STED).²⁰ While NSOM is sensitive enough to image single molecules and can, in principle, reach very high spatial resolutions (the limit is predicted to be ~ 15 nm), it has the disadvantages that it can only be used on surfaces, it suffers from topography-induced image artifacts, and it has seen limited success when applied to very soft samples. The PSF describes the 3D energy density in space measured from a pointlike light-emitting object, and PSF engineering using STED is very promising. However, it is not yet clear whether the method can be sensitive enough to image single molecules.

Two molecules are said to be colocalized when they are separated by less than the optical resolution limit of ~ 250 nm. Colocalization of biomolecular building blocks is often determined by staining the constituents with fluorescent labels that can be separated, at least partially, in their emission spectra. Quantitative 3D fluorescence analysis is performed with multicolor confocal laser scanning microscopy (CLSM) and advanced image analysis techniques.^{21,22} Spherical and chromatic aberrations in the excitation and detection paths diminish the attainable accuracy in multicolor far-field optics-based approaches.^{23,24} To circumvent these problems, Lacoste et al.²⁵ presented a new method for ultrahigh-resolution multicolor colocalization, which relies on the use of luminescent nanoparticles that can be excited by a single laser wavelength but emit at different wavelengths. In combination with multicolor CLSM with "orthogonal" detection channels, the fluorescence of different emitters is separated and recorded independently. Because the same laser excites all emitters, chromatic aberrations in the excitation arm are eliminated. The method was demonstrated using two types of fluorescent nanoparticles, energy-transfer fluorescent beads (TransFluoSpheres) and semiconductor nanocrystal quantum dots (QDs). The large size (20–40 nm) of energy-transfer beads prevents their use for colocalization experiments in small molecular machines. Semiconductor nanocrystal QDs²⁶ are much smaller (2–6 nm), have bright fluorescence, and are far more stable than conventional dyes.²⁷ However, these are not yet widely available, and the possibilities for coupling the particles specifically to biomolecules are extremely limited in comparison with more developed fluorescent dye labeling techniques. An additional drawback of QDs

is that they exhibit intermittent dark periods, a phenomenon referred to as blinking.²⁸ These dark periods deteriorate the quality of images produced using CLSM and result in a reduced precision of localization.^{25,29}

To date, only multicolor colocalization of single fluorescent probes has been demonstrated. As proposed by Betzig in 1995,³⁰ any optically distinguishable characteristic can be used for identification and isolation of a chromophore. For example, it has been shown that the fluorescence lifetime of single fluorescent dyes can be used as an unequivocal identification property.^{31–33} Hence, colocalization of different emitters can also be performed by applying time-resolved fluorescence spectroscopy. The use of fluorescence lifetime as the identification criterion, e.g., two dyes that exhibit similar absorption and emission characteristics but distinct fluorescence lifetimes, simplifies the experimental setup drastically because only a single detector is required. Furthermore, all chromatic and spherical aberrations are prevented. The characteristics of the fluorescence decays is used to extract the relative contribution of fluorescence intensity from each molecule in the resulting PSF images.

Here, we present a new technique for ultrahigh-resolution colocalization of conventional single fluorescent dyes with nanometer accuracy based on confocal fluorescence lifetime imaging microscopy (CFLIM).^{34,35} The method takes advantage of fluorescent dyes that can be efficiently excited by a single pulsed diode laser emitting at 635 nm but differ in their fluorescence lifetime. To determine the contribution of each dye per pixel in the PSF image, a dynamic pattern weighting method^{36,37} was applied. This allows for the creation of independent images for each dye molecule. To determine the accurate positions of the individual PSFs, two different methods were tested. The first approach relies on the assumption that the resulting zero-order maximum of the PSF images can be modeled by a two-dimensional (2D) Gaussian function. The second is to calculate the center of intensity as the sum of the intensity weighted pixel coordinates; this approach works without any underlying model function. Both methods reveal comparable precision of localization of only a few nanometers.

MATERIALS AND METHODS

Sample Preparation and CFLIM of Single Fluorescent Dyes. Measurements were performed using the carbocyanine dye Cy5 (Amersham Life Science; Braunschweig, Germany), and the rhodamine derivative JF9 (kindly provided by K. H. Drexhage,

(16) Schütz, G. J.; Kada, G.; Pastushenko, V. P.; Schindler, H. *EMBO J.* **2000**, *19*, 892–901.

(17) Sako, Y.; Minoguchi, S.; Yanagida, T. *Nat. Cell Biol.* **2000**, *2*, 168–172.

(18) Hell, S.; Stelzer, E. H. K. *J. Opt. Soc. Am. A* **1992**, *9*, 2159–2166.

(19) Enderle, T.; Ha, T.; Ogletree, D. F.; Chela, D. S.; Magowan, C.; Weiss, S. *Proc. Natl. Acad. Sci. U.S.A.* **1997**, *94*, 520–525.

(20) Klar, T. A.; Jacobs, S.; Dyba, M.; Enger, A.; Hell, S. W. *Proc. Natl. Acad. Sci. U.S.A.* **2000**, *97*, 8206–8210.

(21) Patwardhan, A.; Manders, E. M. M. *Bioimaging* **1996**, *4*, 17–24.

(22) Esa, A.; Edelmann, P.; Kreth, G.; Trakhtenbrot, L.; Amariglio, G.; Rechavi, G.; Hausmann, M.; Cremer, C. *J. Microsc.* **2000**, *199*, 96–105.

(23) Manders, E. M. M. *J. Microsc.* **1997**, *185*, 321–328.

(24) van Oijen, A. M.; Köhler, J.; Schmidt, J.; Brakenhoff, G. J. *Chem. Phys. Lett.* **1998**, *292*, 183–187.

(25) Lacoste, Th. D.; Michalet, X.; Pinaud, F.; Chemla, D. S.; Alivisatos, P.; Weiss, S. *Proc. Natl. Acad. Sci. U.S.A.* **2000**, *97*, 9461–9466.

(26) Alivisatos, A. P. *Science* **1996**, *271*, 933–937.

(27) Banin, U.; Bruchez, M.; Alivisatos, A. P.; Ha, T.; Weiss, S.; Chemla, D. S. *J. Chem. Phys.* **1999**, *110*, 1–7.

(28) Kuno, M.; Fromm, D. P.; Hamann, H. F.; Gallagher, A.; Nesbitt, D. J. *J. Chem. Phys.* **2000**, *112*, 3117–3120.

(29) Michalet, X.; Lacoste, Th. D.; Weiss, S. *Methods* **2001**, *25*, 87–102.

(30) Betzig, E. *Opt. Lett.* **1995**, *20*, 237–239.

(31) Zander, C.; Sauer, M.; Drexhage, K. H.; Ko, D.-S.; Schulz, A.; Wolfrum, J.; Brand, L.; Eggeling, C.; Seidel, C. A. M. *Appl. Phys. B* **1996**, *63*, 517–523.

(32) Sauer, M.; Arden-Jacob, J.; Drexhage, K. H.; Göbel, F.; Lieberwirth, U.; Mühlegger, K.; Müller, R.; Wolfrum, J.; Zander, C. *Bioimaging* **1998**, *6*, 14–24.

(33) Sauer, M.; Ankenbauer, W.; Angerer, B.; Földes-Papp, Z.; Göbel, F.; Han, K. T.; Rigler, R.; Wolfrum, J.; Zander, C. *J. Biotechnol.* **2001**, *86*, 181–201.

(34) Tinnefeld, P.; Buschmann, V.; Herten, D. P.; Han, K. T.; Sauer, M. *Single Mol.* **2000**, *1*, 215–223.

(35) Tinnefeld, P.; Herten, D. P.; Sauer, M. *J. Phys. Chem. A* **2001**, *105*, 7989–8003.

(36) Köllner, M.; Fischer, A.; Arden-Jacob, J.; Drexhage, K. H.; Müller, R.; Seeger, S.; Wolfrum, J. *Chem. Phys. Lett.* **1996**, *250*, 355–360.

(37) Enderlein, J.; Sauer, M. *J. Phys. Chem. A* **2001**, *105*, 48–53.

Universität Gesamthochschule Siegen). The dyes were purified on a RP18 column using a gradient of 0–75% acetonitrile in 0.1 M aqueous triethylammonium acetate (TEAA) prior to use. Samples were prepared by exposing clean cover slides to a 10^{-10} M Cy5/ 10^{-10} M JF9 solution in deionized water. The samples were then rinsed with deionized water and dried under nitrogen.

A detailed description of the setup for fluorescence lifetime imaging microscopy at the single-molecule level was reported previously.^{34,35} Briefly, an inverted microscope (Axiovert 100TV; Zeiss) was equipped with a motor-driven x,y -microscope scanning stage (SCAN 100 \times 100 and MC 2000; Märzhäuser, Wetzlar, Germany). A pulsed diode laser emitting at 635 nm with a repetition rate of 64 MHz (PDL800; Picoquant, Berlin, Germany) was used to excite fluorescence. This laser system provides pulses with duration of less than 100 ps. The circularly polarized laser beam passes an excitation filter and is directed to the microscope objective by a dichroic beam splitter. The average laser power was adjusted to ~ 500 W/cm² (corresponding to a peak intensity of ~ 80 kW/cm²) at the sample. Fluorescence was collected by the same objective, passed through a band-pass filter (675RDF50; Omega Optics, Brattleboro, VT) and imaged through the TV outlet on the bottom of the microscope onto a 50- μ m pinhole oriented directly in front of a single-photon-counting avalanche photodiode (AQR-14; EG&G). For generation of fluorescence lifetime images of single molecules, the signal of the avalanche photodiode was fed into a time-correlated single-photon-counting (TCSPC) PCI card (SPC-430, Becker & Hickl, Berlin, Germany). For synchronization of the scanning motion with fluorescence detection, a Windows 32-based software running under Windows NT was developed with Microsoft Visual C++ 5.0. Fluorescence lifetime images were measured with a resolution of 50 nm/pixel and an integration time of 6 ms/pixel.

Data Analysis. Data analysis was performed with a set of custom software tools written in C and C++. To enable the discrimination of molecules differing in fluorescence lifetime, the TCSPC image data were separated into individual fluorescence intensity images. To assign the contribution of the total intensity of each pixel to each of the two dye types, the lifetime information was used with an algorithm derived from the method of whole pattern matching originally developed for DNA sequencing.^{36–38} The method is based on the log-likelihood ratio estimator LL given in eq 1.

$$LL = \sum_{i=1}^k n_i \ln((n_i/Np_i)) \quad \text{with} \quad N = \sum_{i=1}^k n_i \quad (1)$$

Here, n_i is the number of photons acquired in each channel i running from 1 to k of the measured fluorescence decay and p_i gives the modeled probability to detect a photon in the i th channel. The measured fluorescence decay pattern p (usually the average decay curve for many molecules) can be described as a weighted sum $p(\alpha) = \alpha x + (1 - \alpha) y$ of the fluorescence decay pattern x and y , respectively, of the two chromophores, where α is the relative portion of chromophore X to be estimated. The estimation

was performed by application of the robust simplex-downhill algorithm.³⁹ By using this linear model, we make the assumption that there are no intermolecular interactions between dye molecules that might influence the fluorescence kinetics. In other words, we assume that the two chromophores fluoresce independently of each other. The two resulting images containing the relative portions of each chromophore α and $(1 - \alpha)$, respectively, were multiplied with the values of the total fluorescence intensity image to obtain two separate fluorescence intensity images for the localization analysis. This method has the benefit that no assumptions need be made regarding the fluorescence kinetics of the investigated fluorophores. Using this pattern matching technique means that it is not a requirement that the dyes emit with simple single-exponential fluorescence decays, though in our case they do. Since the model, x and y patterns are all taken from the original TCSPC measurements, even systematic errors, like distortions of the laser pulse, are taken into account automatically.

RESULTS AND DISCUSSION

Currently, colocalization experiments of different chromophores or labeled biomolecules below optical resolution rely on different colors of the dyes used.^{23–25,40} Recently, colocalization and fluorescence resonance energy transfer were observed by simultaneously imaging the emission and polarization characteristics of two colocalized fluorophores using two different laser excitation sources.^{41,42} It should be noted that high-precision position distance measurements (HPDMs) of single molecules are influenced by the photophysical dynamics of the fluorophores used. Fluctuations in the spectroscopic properties such as the emission spectrum or fluorescence lifetime will substantially increase the error in HPDMs.³⁵ In addition, *off* times due to long-lived triplet states will generate patchy PSFs, which also deteriorate the precision of the position determination. This means that the fluorescent dyes used for HPDMs should not only be sufficiently photostable and bright, but should also exhibit triplet *off* times that are much shorter than the integration time per pixel used in the experiments. A further requirement is that the dyes should show homogeneous fluorescence lifetime characteristics; i.e. for fluorescence lifetime-based HPDMs, the dyes used should show single-molecule fluorescence lifetime distributions with single maximum and minimum overlap. In our experiments, the dye molecules were coated directly onto untreated glass surfaces. The adsorption of relatively planar chromophores onto a smooth glass surface is expected to take place homogeneously with an almost planar orientation of the chromophore on the surface. Several reports have discussed the effect of dipole orientation of dyes molecules on the expected and measured radiative lifetimes due to electromagnetic boundary conditions.^{43,44}

JF9, a rhodamine derivative, and Cy5, a carbocyanine derivative, are a suitable combination of dyes for HPDMs using single-

(38) Lieberwirth, U.; Arden-Jacob, J.; Drexhage, K. H.; Hertel, D. P.; Müller, R.; Neumann, M.; Schulz, A.; Siebert, S.; Sagner, G.; Klingel, S.; Sauer, M.; Wolfrum, J. *Anal. Chem.* **1998**, 70, 4771–4779.

(39) Press, W. H.; Teukolsky, S. A.; Vetterling, W. T.; Flannery, B. P. *Numerical Recipes in C*, 2nd ed.; Cambridge University Press: New York, 1994.

(40) Esa, A.; Edelmann, P.; Kreth, G.; Trakhtenbrot, L.; Amariglio, G.; Rechavi, G.; Hausmann, M.; Cremer, C. *J. Microsc.* **2000**, 199, 96–105.

(41) Cognet, L.; Harms, G. S.; Blab, G. A.; Lommerse, P. H. M.; Schmidt, T. *Appl. Phys. Lett.* **2000**, 77, 4052–4054.

(42) Trabesinger, W.; Hecght, B.; Wild, U. P.; Schütz, G. J.; Schindler, H.; Schmidt, Th. *Anal. Chem.* **2001**, 73, 1100–1105.

(43) Drexhage, K. H. *J. Luminesc.* **1970**, 1, 2, 693–701.

(44) Macklin, J. J.; Trautman, T. D.; Harris, T. D.; Brus, L. E. *Science* **1996**, 272, 255–258.

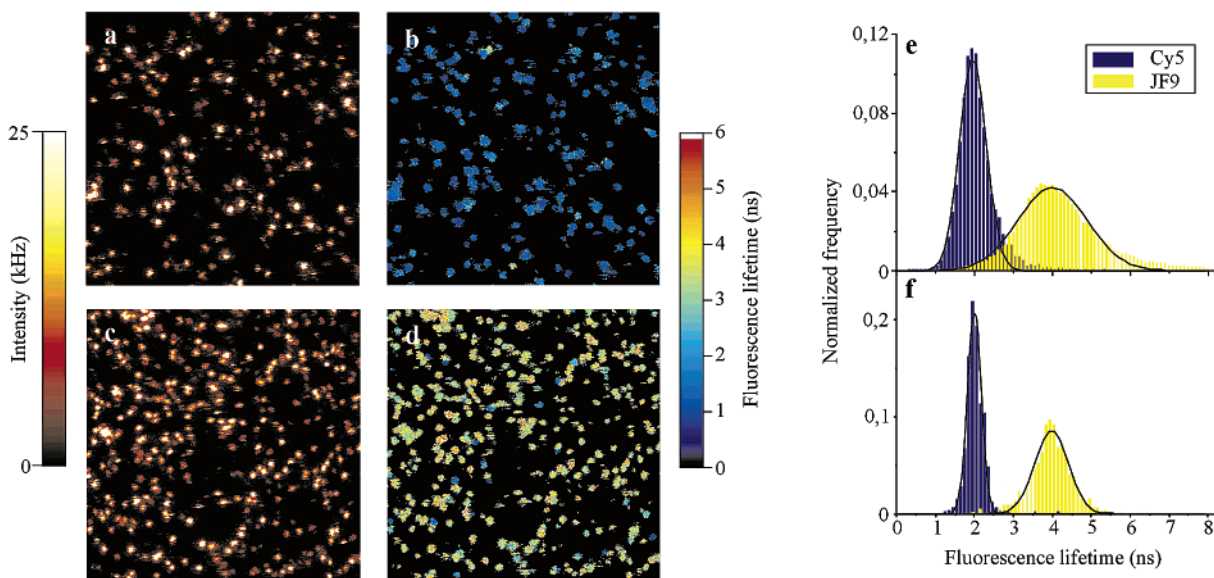


Figure 1. Fluorescence intensity and lifetime confocal images ($17 \times 17 \mu\text{m}$) of single Cy5 (a, b) and JF9 molecules (c, d) on a glass surface (6-ms integration time per pixel; excitation power, 500 W/cm^2). The surface was scanned from top to bottom and from left to right with a resolution of 50 nm/pixel . In the resulting fluorescence lifetime images, pixels corresponding to count rates of less than 3 kHz were excluded. Normalized histograms of pixel-integrated (e) and spot-integrated (f) fluorescence lifetimes of single JF9 and Cy5 molecules obtained from separate experiments using glass surfaces with only one class of dye molecules.

molecule colocalization based solely on different fluorescence lifetimes. The two dyes exhibit a 2-fold difference in fluorescence lifetime when adsorbed on a dry glass surface. JF9 has a fluorescence lifetime of $\sim 4 \text{ ns}$, and Cy5 has a fluorescence lifetime of $\sim 2 \text{ ns}$.³⁵ Both of these dye types exhibit short triplet lifetimes of $2\text{--}7 \mu\text{s}$ for JF9 and $0.01\text{--}5 \text{ ms}$ for Cy5 adsorbed on bare glass surfaces under air-equilibrated conditions.³⁵ In addition, the two chromophores can be efficiently excited using a single pulsed 635-nm laser diode and exhibit similar emission maximums.

Panels a and c of Figure 1 show scanning confocal fluorescence intensity images of single Cy5 and JF9 molecules, respectively, adsorbed on cover slides. The images exhibit diffraction-limited spots with count rates of up to 30 kHz . With a background count rate of 1.5 kHz signal-to-background ratios (S/B) of up to 20 were calculated for the most intense pixels in our experiments. For both chromophores, an average of ~ 4000 photon counts were detected per single-molecule spot. Using an integration time of 6 ms/pixel , the PSF images of most single molecules appear homogeneous and show few isolated dark pixels. The fluorescence lifetime images shown in Figure 1b and d were calculated from the photon counts collected per pixel using a maximum likelihood estimator (MLE) algorithm.^{34,35} To suppress the background efficiently, pixels corresponding to count rates of less than 3 kHz , i.e., less than 18 photon counts, were excluded. While the two chromophores exhibit similar count rates, there are substantial deviations in fluorescence lifetimes measured from single molecules compared to the average values. To quantify the homogeneity of the fluorescence lifetimes, we calculated the pixel- and spot-integrated fluorescence lifetimes for more than 400 single JF9 and Cy5 molecules. The resulting distributions of fluorescence lifetimes were each fit to a Gaussian function (Figure 1e,f). Although it is expected that the dielectric interface will modify the radiative component of the excited-state lifetime of the chromophores,^{43,44} the measured fluorescence lifetime distribu-

tions are rather narrow with 1.99 ± 0.67 (pixel-integrated) and $2.00 \pm 0.34 \text{ ns}$ (spot-integrated) for single Cy5 and 4.00 ± 1.72 (pixel-integrated) and $4.00 \pm 0.84 \text{ ns}$ (spot-integrated) for single JF9 molecules. The broader distributions in the case of pixel-integrated fluorescence lifetimes clearly result from the lower number of photon counts per decay (fluorescence lifetimes were calculated from 18 to 180 photon counts). The relatively homogeneous distributions indicate that most molecules take a more or less pronounced planar orientation on dry glass surface. The high identification accuracy of the two chromophores due to their different excited-state kinetics makes possible the fluorescence lifetime-based high-precision distance measurements.

Panels a and b of Figure 2 show a fluorescence intensity and lifetime image, respectively, measured from a 1:1 mixture of JF9 and Cy5 molecules adsorbed on a cover slide. The fluorescence lifetime image (Figure 2b) constructed via the MLE algorithm clearly indicates the existence of the two chromophores randomly distributed on the glass surface. By their random spatial distribution on the surface, some JF9 and Cy5 molecules are colocalized within the same PSF. To separate the PSFs of two colocalized chromophores, information about the contribution of each chromophore per pixel is required. Due to the low number of photon counts in single-molecule experiments, especially at the fringe regions of the PSFs, a modified whole pattern matching method^{36,37} was applied to recalculate the contribution of different fluorescence decay patterns to a measured fluorescence decay. As already described under Materials and Methods, this method uses a fluorescence decay pattern taken from separate experiments of the contributing dyes under exactly the same experimental conditions. Figure 3 shows the two spot-integrated fluorescence decays used as model patterns to estimate the contribution of each dye in a colocalized PSF image. The model decay patterns were obtained by averaging 50 spot-integrated single-molecule decays selected from images containing only one class of dye. The two

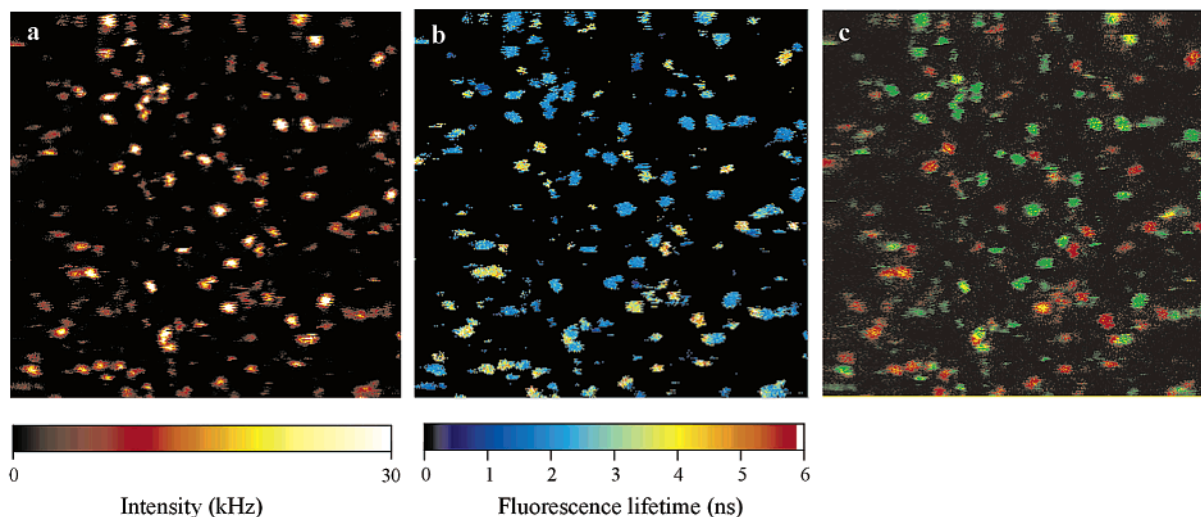


Figure 2. (a) Fluorescence intensity, (b) fluorescence lifetime, and (c) false color image ($15 \times 15 \mu\text{m}$) of randomly distributed dye molecules Cy5 and JF9 on a glass surface (6-ms integration time per pixel; excitation power, 500 W/cm^2). The surface was scanned from top to bottom and from left to right with a resolution of 50 nm/pixel . The false color image was obtained by applying the pattern matching technique and subsequent data processing described in the text.

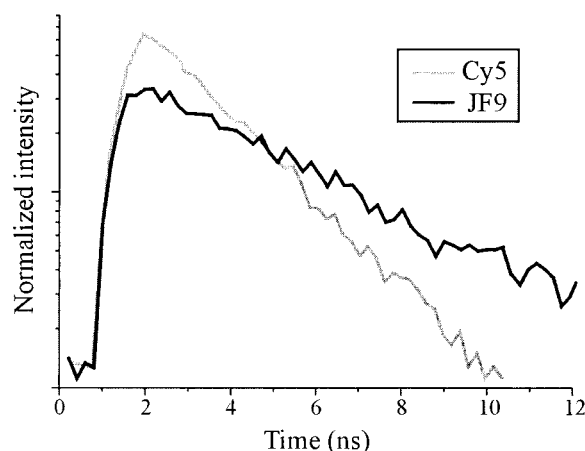


Figure 3. Model fluorescence decay patterns of Cy5 and JF9 molecules adsorbed on dry glass surface used for the calculation of the contribution of each dye per spot. The decay patterns are obtained by averaging 50 spot-integrated single-molecule fluorescence decays of each dye type. They can be satisfactorily fit using a monoexponential model with lifetimes of 2.0 (Cy5) and 4.0 ns (JF9).

decay patterns were used for the estimation of the contribution of each dye per pixel to create two distinct fluorescence intensity images containing the relative portion of the dyes. The resulting images were multiplied with the total fluorescence intensity from the original image (Figure 2a) to construct two intensity-weighted images. For parallel visualization each of the intensity-weighted image was assigned a color channel of a red–green–blue (RGB) image and merged into the resulting false color image shown in Figure 2c. Hence, green spots represent the absolute contribution of Cy5 molecules while red spots represent JF9 molecules. Overlapping PSFs are indicated by intermediate shades of yellow (Figure 3c).

An important prerequisite to measure distances is the exact localization of a fluorescent molecule. Generally, the PSF of a pointlike light source can be approximated by a 2D Gaussian

function⁴⁵ (eq 2).

$$I(x,y) = I_0 + A \exp\left(\frac{-(x-x_s)^2}{2\sigma_x^2}\right) \exp\left(\frac{-(y-y_s)^2}{2\sigma_y^2}\right) \quad (2)$$

Another possibility to localize the intensity center of a PSF image is based on the normalized weighted intensities (eq 3).

$$\begin{pmatrix} x_s \\ y_s \end{pmatrix} = \frac{\sum_{x=x_0}^{x_{\max}} \sum_{y=y_0}^{y_{\max}} (x) I(x,y)}{\sum_{x=x_0}^{x_{\max}} \sum_{y=y_0}^{y_{\max}} I(x,y)} \quad (3)$$

In the case of a circularly symmetric and nonpatchy PSF, both methods are expected to reveal similar results. We applied the center-of-mass method and a 2D Gaussian fit to calculate the fluorescence intensity centers of more than 100 different PSF images of single Cy5 and JF9 molecules that showed no evidence of strong blinking. The differences between the calculated center positions using the two methods were always smaller than 4 nm in both the directions (i.e., the fast and slow scan axes). This implies that, for relatively homogeneous fluorescent spots and high S/B ($S/B > 10$), either method can be used with comparable results.⁴⁶ Due to the shorter computation time of the center-of-mass method, this method was used for locating PSF center positions for the data presented.

Figure 4 shows two examples of colocalized JF9 and Cy5 molecules with calculated distances of 204 ± 21 and $42 \pm 18 \text{ nm}$, respectively. The error in the calculated center of mass of the weighted intensity images, I_w (Figure 4b,c and f,g) is determined

(45) Schmidt, T.; Schütz, G. J.; Baumgartner, W.; Gruber, H. J.; Schindler, H. *Proc. Natl. Acad. Sci. U.S.A.* **1996**, *93*, 2926–2929.

(46) Cheezum, M. K.; Walker, W. F.; Guilford, W. H. *Biophys. J.* **2001**, *81*, 2378–2388.

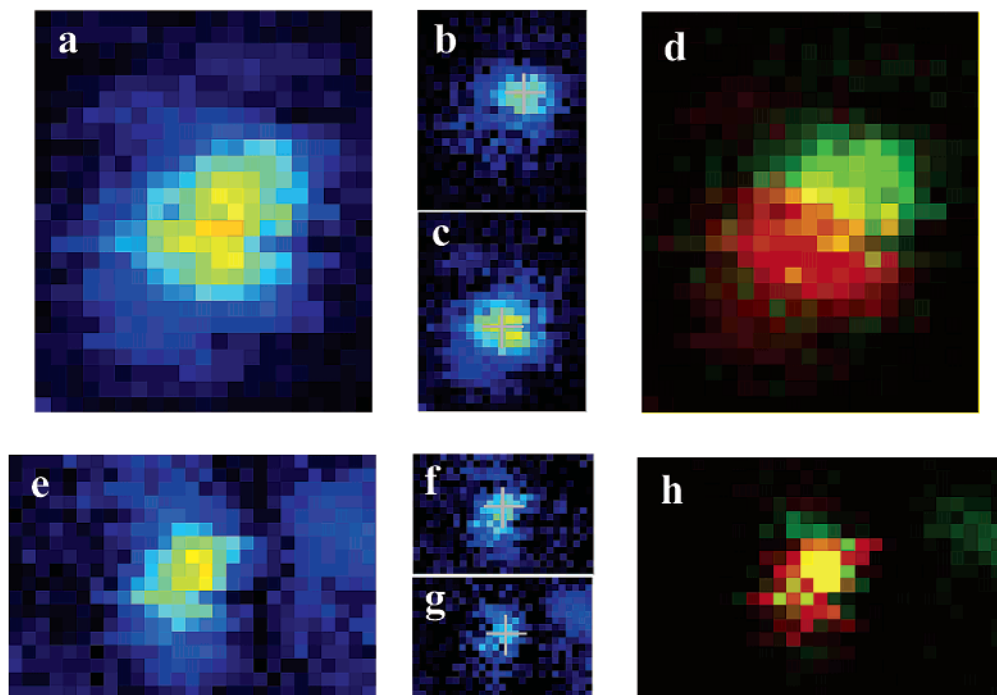


Figure 4. Colocalization of single JF9 and Cy5 molecules with distances of 204 ± 21 (a–d) and 42 ± 18 nm (e–h). The two decay patterns shown in Figure 3 were used for the estimation of the contribution of each dye in the fluorescence intensity images (a, e) to create two distinct fluorescence intensity images containing the relative portion of the dyes. The resulting JF9 images (b, f) and Cy5 images (c, g) were multiplied with the fluorescence intensity of the original images to construct false-color images (d, h).

by (1) the contribution, $\alpha_{x,y}$, of the two chromophores provided by whole pattern matching and (2) the total number of photons acquired in each pixel, I_T , using $I_w = \alpha_{x,y}I_T$. We assume that only shot noise contributes to the error in the number of photon counts per pixel. Therefore, the error in photon counts I at a pixel x, y is given by eq 4.

$$\Delta I_{x,y} = \sqrt{I_{x,y}} \quad (4)$$

The error of the contribution, $\Delta\alpha_{x,y}$, per pixel, x, y , provided by whole pattern matching can be estimated using eqs 5 and 6 by

$$\overline{\tau_{x,y}} = \alpha_{x,y}\tau_1 + (1 - \alpha_{x,y})\tau_2 \quad (5)$$

$$\alpha_{x,y} = \frac{\overline{\tau_{x,y}} - \tau_2}{\tau_1 - \tau_2} \quad (6)$$

comparison of the centers of the fluorescence lifetime distributions (2 ns for Cy5 and 4 ns for JF9) with the average fluorescence lifetime of the raw data, $\overline{\tau_{x,y}}$, calculated via the MLE algorithm.

The error of the MLE estimation of the average fluorescence lifetime of the raw data is 1 order of magnitude smaller than the standard deviations of the pixel-integrated fluorescence lifetime distributions. Therefore, $\Delta\alpha_{x,y}$ can be derived from the standard deviations of the pixel-integrated fluorescence lifetime distributions (Figure 1e) using eq 6 and a Gaussian error propagation.

Figure 5 shows several determined distances between single colocalized JF9 and Cy5 molecules adsorbed on a glass surface in the distance range 25–80 nm and the corresponding relative errors. Figure 5 shows that the relative error in distance deter-

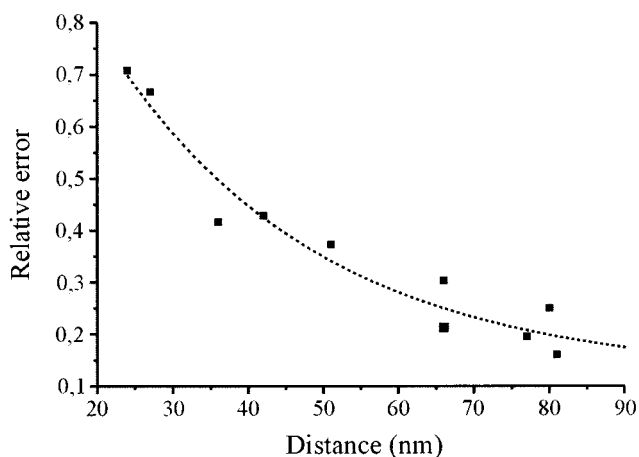


Figure 5. Relative error in calculated distances between colocalized single JF9 and Cy5 as a function of the separation distance in the range 25–80 nm.

mination is significant when the two molecules are less than 40 nm apart. Hence, a barrier of ~ 40 nm in fluorescence lifetime-based single-molecule HPDMs must presently be accepted. However, it should be pointed out that the error in distance determination is strongly controlled by the fluorescence lifetime difference of the two chromophores, the number of detected fluorescence photons per single chromophore, and the background count rate.^{47–50} Although autofluorescence is reduced in

(47) Enerlein, J. *Exp. Tech. Phys.* **1991**, 39, 479–486.

(48) Köllner, M.; Wolfrum, J. *Chem. Phys. Lett.* **1992**, 200, 199–203.

(49) Köllner, M. *Appl. Opt.* **1993**, 32, 806–820.

(50) Thompson, R. E.; Larson, D. R.; Webb, W. W. *Biophys. J.* **2002**, 82, 2775–2783.

the red spectral region, it is difficult to completely get rid of elastic and inelastic scattering in single-molecule experiments. On the other hand, the S/B and lifetime difference between the two chromophores might be improved by the use of an optimized chromophore pair. We are currently in the process of performing single-molecule colocalization experiments and simulations to study the influence of the fluorescence lifetime difference and S/B on the error in distance determination.

CONCLUSIONS

We presented a new method to determine the distance between single, conventional dye molecules well below the optical resolution limit of confocal fluorescence microscopy using fluorescence lifetime information as the sole discrimination criterion. By the use of appropriately selected fluorescent dyes, the method allows one to measure intermolecular distances down to ~ 40 nm with an error of ~ 18 nm free of any chromatic aberrations. The presented results demonstrate that fluorescence lifetime-based high-precision distance measurements open new possibilities for colocalization experiments between single molecules. To further increase the precision in distance determination, that is, to enable

the measurement of shorter distances, several improvements are possible. First, higher photon count statistics per dye or larger differences in fluorescence lifetime would definitely improve the localization accuracy. Second, by combining different spectroscopic characteristics, such as the simultaneous measurement of fluorescence lifetime, emission spectrum, and fluorescence polarization, one could greatly enhance localization accuracy in distance determination.³⁵

ACKNOWLEDGMENT

The authors thank K. H. Drexhage for the generous disposal of the rhodamine derivative JF9. Financial support by the Deutsche Forschungsgemeinschaft (Grant Cr60/16-2) and the Bundesministerium für Bildung, Wissenschaft, Forschung und Technologie (Grant 311864) is gratefully acknowledged.

Received for review February 11, 2002. Accepted April 25, 2002.

AC025576G